

Journal of Geophysical Research: Biogeosciences

RESEARCH ARTICLE

10.1029/2017JG004285

Special Section:

Biogeochemistry of Natural Organic Matter

Key Points:

- Age dynamics of particulate organic matter in Changjiang (Yangtze River) were investigated by $\Delta^{14}\text{C}$ values
- The contributions of biomass and pre-aged soil organic matter were dominant, regardless of the hydrological conditions
- Dam effect and retention of fresh organic matter in the lower reaches has modified the organic matter age and composition

Supporting Information:

- Supporting Information S1

Correspondence to:Y. Wu,
wuying@sklec.ecnu.edu.cn**Citation:**Wu, Y., Eglinton, T. I., Zhang, J., & Montlucon, D. B. (2018). Spatiotemporal variation of the quality, origin, and age of particulate organic matter transported by the Yangtze River (Changjiang). *Journal of Geophysical Research: Biogeosciences*, 123, 2908–2921. <https://doi.org/10.1029/2017JG004285>

Received 6 NOV 2017

Accepted 9 AUG 2018

Accepted article online 22 AUG 2018

Published online 15 SEP 2018

Spatiotemporal Variation of the Quality, Origin, and Age of Particulate Organic Matter Transported by the Yangtze River (Changjiang)

Ying Wu¹ , Timothy I. Eglinton^{2,3} , Jing Zhang¹, and Daniel B. Montlucon^{2,3}

¹State Key Laboratory of Estuarine and Coastal Research, East China Normal University, Shanghai, China, ²Department of Marine Chemistry and Geochemistry, Woods Hole Oceanographic Institution, Woods Hole, MA, USA, ³Geological Institute, Department of Earth Sciences, ETH Zurich, Zurich, Switzerland

Abstract Information on the age dynamics of particulate organic matter (POM) in large river systems is currently sparse and represents an important knowledge gap in our understanding of the global carbon cycle. Here we examine variations in organic geochemical characteristics of suspended sediments from the Changjiang (Yangtze River) system collected between 1997 and 2010. Higher particulate organic carbon content (POC%) values were observed in the middle reach, especially after 2003, and are attributed to the increase of in situ (aquatic) primary production associated with decreased total suspended matter concentrations. Corresponding $\Delta^{14}\text{C}$ values from depth profiles taken in 2009 and 2010 indicate spatial and temporal variations in POC sources within the basin. Two isotopic mass balance approaches were explored to quantitatively apportion different sources of Changjiang POM. Results indicate that contributions of biomass and pre-aged soil organic matter are dominant, regardless of hydrological conditions, with soil-derived organic carbon comprising 17–56% of POC based on a Monte Carlo three-end-member mixing model. In contrast, binary mixing model calculations suggest that up to 80% of POC (2009 samples only) derived from biospheric sources. The emplacement of the Three Gorges Dam and resulting trapping of sediment from the upper reach of the watershed resulted in a modification of POM ^{14}C ages in the reservoir. With the resulting decline in sediment load and increase in the proportion of modern POC in the lower reach, these changes in POM flux and composition of the Changjiang have significant implications for downstream carbon cycle processes.

1. Introduction

Understanding the controls on fluxes and dynamics of processes associated with fluvial transfer of terrestrial organic carbon (OC) from the continents to the ocean represents a fundamental challenge for carbon cycle biogeochemists (Aufdenkampe et al., 2011; Battin et al., 2009; Benner, 2004; Hedges et al., 1997; Goñi et al., 1997, 1998, 2005; Tranvik et al., 2009). In particular, whether these processes result in a net source or sink of atmospheric CO_2 depends on both the fate of terrestrial OC in the marine environment and on the origin and nature of the exported carbon (Eglinton & Eglinton, 2008; Feng et al., 2013; Galy & Eglinton, 2011; Rosenheim et al., 2013). Rivers are integral and dynamic components of the global carbon cycle, transporting, storing, and processing huge amounts of OC supplied from surrounding watersheds, as well as produced within the fluvial network (Aufdenkampe et al., 2011; Borges et al., 2015; Marwick et al., 2015; Raymond et al., 2004; Schefuss et al., 2016). However, a comprehensive understanding of the factors that influence the composition, reactivity, and mobilization of terrestrially derived OC within river basins is still lacking.

River systems are becoming increasingly affected by human activities such as dam construction, deforestation and agriculture, water diversion, and sand mining (Bianchi & Allison, 2009; Yang et al., 2015). Large-scale alterations to the hydrological plumbing of rivers have changed the fluxes and ratios of carbon and nutrients, as well as the proportions of dissolved versus particulate materials, reaching coastal waters (Bao et al., 2015; Wu et al., 2015). Large river systems developed on passive margins have significant capacity to store eroded sediments. Extended residence times in intermediate reservoirs, such as floodplains, wetlands, and dam systems, result in modification of the composition and structure of transported organic material, and such systems can also act as a source of CO_2 to the atmosphere (Bao et al., 2015; Battin et al., 2009; Blair & Aller, 2012; Liu et al., 2016). Understanding these various controls (especially the effect of dam construction on particles)

on the residence time and fate of terrestrial organic matter (OM) in river basins in the face of ongoing climatic change and anthropogenic disturbance therefore constitutes an important challenge.

A number of studies have measured the radiocarbon compositions of bulk OC or specific plant-derived biomarkers in sedimentary deposits or total suspended matter (TSM) with the aim of constraining the ages and sources of terrestrial OM within river basins and its relationships with OM burial on continental margins (Blair & Aller, 2012; Feng et al., 2013; Galy & Eglinton, 2011; Marwick et al., 2015; Schefuss et al., 2016; Tao et al., 2015). Measured radiocarbon ages of riverine OC are generally interpreted as the mean time elapsed since biosynthesis and are taken to reflect the integrated effects of transit, as well as temporary deposition and storage of carbon within the watershed (Goñi et al., 2005; Marwick et al., 2015; Rosenheim & Galy, 2012). Further insights into carbon sources and cycling within river systems can be gained when radiocarbon observations are used in combination with $\delta^{13}\text{C}$ measurements (Goñi et al., 2005; Marwick et al., 2015; Schefuss et al., 2016; Tao et al., 2015). At the global scale, the median $\Delta^{14}\text{C}$ value of bulk particulate OC (POC) was found to be -203‰ , corresponding to an age of $\sim 1,800$ years (Marwick et al., 2015). Younger POC ages have been observed in tropical rivers, whereas older ages have been detected in temperate and higher-latitude regions with a larger influence of geomorphology and soil erosion (Feng et al., 2013; Galy & Eglinton, 2011; Leithold et al., 2006; Li et al., 2015; Longworth et al., 2007; Moreira-Turcq et al., 2013; Schefuss et al., 2016; Tao et al., 2015; Wang et al., 2012). Given that anthropogenic activities such as dam construction modify both the location and timescales of storage of OM within river basins (Li et al., 2015), it is important to establish and determine characteristics of different specific river systems in order to understand their natural dynamics and to predict human influences on underlying biogeochemical processes (Tao et al., 2015). Studies examining carbon isotopic (especially radiocarbon) characteristics of POC under different hydrological conditions within large river basins remain scarce. Such information is vital for assessment of the factors controlling spatial and temporal variability in riverine OM content and composition.

The Changjiang (Yangtze River) is a globally significant fluvial system. Beginning approximately 55 million years ago, the Changjiang drainage basin has fed a main tributary that is distinctive in terms of both the extent of its catchment area and associated global water and chemical fluxes into the ocean. Within the last century, the Changjiang has also experienced heavy anthropogenic disturbance, including the construction of Three Gorges Dam (TGD), the world's largest hydropower project, which was coffer-dammed in 1997, began operation in 2003, and was fully operational in 2006. Sediment decline associated with dam emplacement carries important biogeochemical implications. There have been numerous studies of the biogeochemical characteristics of OM and human impacts on the river with bulk proxies and lignin phenols, which have successfully elucidated the effect of dam construction on the composition and structure of particulate OM (POM; e.g., Bao et al., 2015; Dai et al., 2014; Wu et al., 2007, 2015; Yang et al., 2006, 2011, 2015; Yu et al., 2011; Zhang et al., 2014). However, there is currently very limited available information on the age of OM, particularly in the lower reach downstream of TGD only (Li et al., 2015; Wang et al., 2012). Further knowledge of OM storage and modification in the Changjiang system, especially in basin size and different hydrological conditions, would shed light on potential natural and/or anthropogenic controls (e.g., TGD construction) on the balance between OM export and burial versus respiration, leading to a better understanding of carbon cycle processes on both regional and global scales.

In this study, we present the results from multiyear observations in the Changjiang basin, focusing on the seasonal variability of POC concentration (expressed as the carbon content of TSM), chlorophyll-a (Chl-a), and $\delta^{13}\text{C}$ values. POC ages of depth profile samples are also examined under different hydrological conditions. This first basin-wide study of OM ages in the Changjiang provides a framework for better understanding (controls on) spatial and temporal variations in OM sources (Ganges—Galy & Eglinton, 2011; Amazon—Bouchez et al., 2014; Mackenzie—Hilton et al., 2015); in addition, the effect of TGD construction on the quality, origin, and ages of particles are evaluated.

2. Materials and Methods

2.1. Study Area

The Changjiang is the world's fourth longest river ($\sim 6,300$ km), originating from the Qinghai-Tibetan Plateau at an altitude of more than 5,000 m. The upper reach covers the region of the Jinshajiang River basin, Sichuan Province, and the Three Gorges Reservoir (TGR), the latter modulating present sediment supply to the

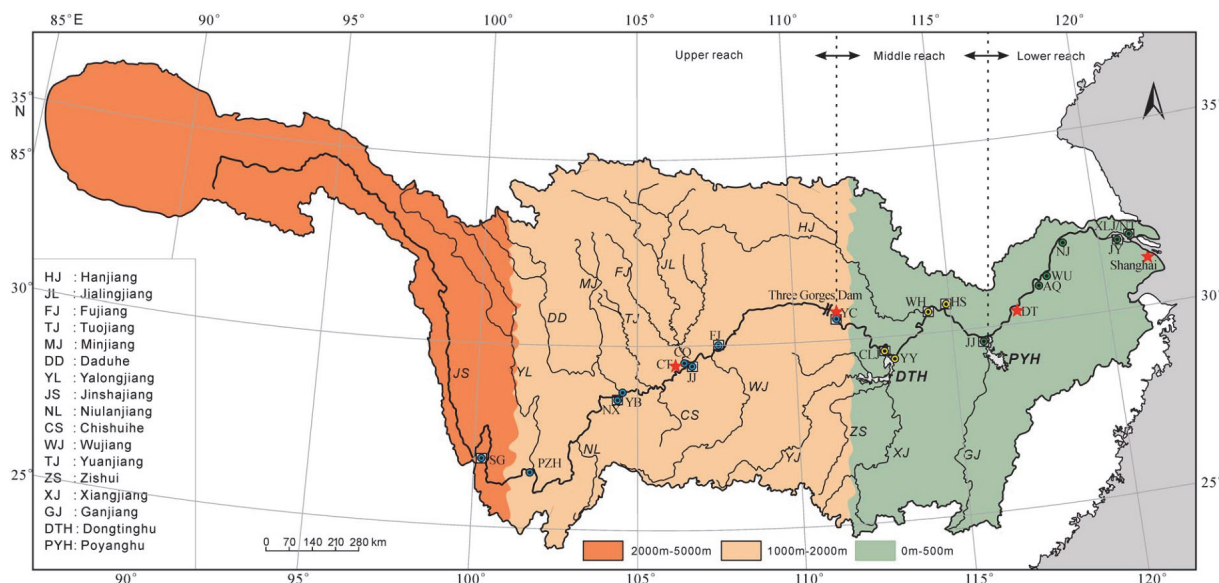


Figure 1. Watershed and tributaries of Changjiang, showing the observational and major sampling sites sampled during field expeditions between 1997 and 2010 (for a full list of sampling stations, please refer to Table S1). Explanation of the tributary and sampling station abbreviations are listed in Table 2. Star symbol represents gauge stations, and different colors represent samples collected from different reaches (blue represents upper reach, yellow marks middle reach, and green for lower reach). Square marking means ^{14}C data available in 2009 or 2010.

mainstem. The middle reach begins at Yichang (YC; elevation 100–2,400 m) and meanders through a fluvial plain and two large lake systems that interact closely with the mainstem. The lower reach begins at Hukou (the outlet of Poyang Lake, elevation ~32 m), below which no large tributaries join the river (Figure 1). The end of the lower reach is Xuliujiang, which is about 125 km from the coast. The uppermost location of the river that is free of tidal influence is called Datong (DT), where the hydrological station is located.

2.2. Sample Collection

Since 1997, we have been conducting six expeditions upstream from the river mouth in order to assess biogeochemical characteristics of the Changjiang under different hydrographic regimes (Table 1 and supporting information Table S1). During three campaigns, samples were collected over ~4,200-km span of the river along the mainstem, including sampling of 15 major tributaries. Other expeditions mainly focused on the middle and lower reaches, from the TGD to the river mouth (Figure 1). Depth profile samples were collected from the river during the 2009 survey. Surface water samples (<1 m) were obtained using an acid-cleaned bucket that was prerinse with in situ water. Depth profile samples were collected using 5-L Niskin bottles attached to nylon cables, and samples of bottom water were taken ~1 m above the riverbed.

Filtration was carried out immediately in the field through precombusted 0.7- μm glass fiber filters (47-mm diameter) for POC, Chl- α , and isotopic analyses. All samples were stored in precombusted foil at -20°C prior to analysis. TSM was calculated from the dry weight of the filtered material captured on the filters. Radiocarbon measurements were performed on bulk POM samples from the 2009 and 2010 campaigns. During the 2009 sampling campaign, the TGR was in a period of impoundment, and the average water discharge at DT ($\sim 17,000 \text{ m}^3 \text{ s}^{-1}$) corresponds to among the lowest measured discharge values (Figure 2a). This sampling period was thus regarded as representative of low-discharge conditions. The water discharge at DT during the 2010 survey was $\sim 61,450 \text{ m}^3 \text{ s}^{-1}$, and the 2010 flood was reported to be the largest in the last decade (Bao et al., 2015).

2.3. Analytical Methods

The filters for POC analysis and sediment samples were dried at 55°C in the lab. Particles were carefully scraped off the filters for further analysis. Sediments were ground and sieved (80 mesh, 178 μm) before further analysis. Carbonate removal prior to OC% and stable carbon isotope and radiocarbon analysis of POC was achieved by acid fumigation with concentrated HCl (Wu et al., 2015). An aliquot of each sample

Table 1
General Geochemical Characteristics of Particulate Organic Matter Collected Between 1997 and 2010 in the Changjiang Watershed

Period	Site	No. of stations	TSM (mg/L)	POC (%)	POC (mg/L)	$\delta^{13}\text{C}_{\text{org}}$ (‰)	Chl- <i>a</i> (µg/L)
Apr 1997	River		80.6	1.2	1.0	-25.6	
	Upper reach	12	81.2	1.2	1.1	-25.5	
	Middle reach	6	97.6	1.1	1.1	-25.7	
	Lower reach	8	67.1	1.0	0.7	-25.6	
Apr 2003	River		65.9	1.1	0.6	-24.7	4.5
	Upper reach	6	41.0	1.2	0.4	-24.6	3.4
	Middle reach	3	93.9	1.0	0.9	-24.8	4.7
	Lower reach	4	82.2	0.9	0.8	-24.9	6.1
Nov 2006	River		33.6	2.8	0.7		5.3
	Upper reach						
	Middle reach	6	19.3	3.8	0.5		6.1
	Lower reach	7	49.9	1.8	0.8		4.4
Jan 2008	River		45.5	2.0	0.7	-25.1	
	Upper reach						
	Middle reach	10	21.6	2.5	0.4	-25.3	
	Lower reach	8	74.7	1.4	1.0	-24.9	
Oct 2009	River		199.2	0.7	1.0	-24.4	0.7
	Upper reach	6	316.3	0.5	1.5	-22.9	0.4
	Middle reach	3	33.7	1.1	0.3	-24.3	0.7
	Lower reach	4	47.6	1.0	0.5	-25.3	1.2
Jun 2010	River		40.2	2.0	0.6		2.4
	Upper reach						
	Middle reach	4	30.8	2.3	0.6	-26.9	3.3
	Lower reach	5	47.8	1.7	0.7	-26.2	1.6
Jul 2010	River		226.9	1.2	2.6	-25.0	
	Upper reach						
	Middle reach	3	266.8	1.2	3.1	-24.8	
	Lower reach	6	146.9	1.1	1.6	-25.3	

Note. Average values of TSM (mg/L), POC content (%) and concentration (mg/L), stable isotopic composition ($\delta^{13}\text{C}$, ‰), and Chl-*a* concentration (µg/L) for the different regions are listed for comparison. Average values of each campaign were summarized in the rows of "River." TSM = total suspended matter; POC = particulate organic carbon; Chl-*a* = chlorophyll-*a*.

was used for POC and bulk stable carbon isotope ($\delta^{13}\text{C}$) analyses at the National Ocean Sciences Accelerator Mass Spectrometry (NOSAMS) Facility at Woods Hole Oceanographic Institution. Bulk ^{14}C analysis was also conducted at NOSAMS using established protocols (e.g., Gustafsson et al., 2011). The ^{14}C data are reported as percentage modern carbon and $\Delta^{14}\text{C}$ (‰) values after correction for ^{13}C fractionation (normalization to $\delta^{13}\text{C} = -25\text{‰}$). Chl-*a* for particulate samples were extracted using acetone (90%), determined using a spectrophotometer, and concentrations were calculated using the Lorenzen (1967) equations.

2.4. Two Models Applied to Assess Different Origins of POM

The binary mixing model was applied to estimate the proportions of petrogenic and biospheric contributions ($\text{POC}_{\text{petro}}$ and POC_{bio} , respectively), which can be described by the following governing equations (Galy et al., 2008; Galy & Eglinton, 2011):

$$f_{\text{biosphere}} + f_{\text{petro}} = 1 \quad (1)$$

$$f_{\text{biosphere}} \times A_{\text{biosphere}} + f_{\text{petro}} \times A_{\text{petro}} = A_{\text{sample}} \quad (2)$$

where $f_{\text{biosphere}}$ and f_{petro} are the fractions of POC derived from biospheric and petrogenic sources, respectively; A_{sample} is the measured composition of riverine POC samples; and $A_{\text{biosphere}}$ and A_{petro} are the compositions of biospheric and petrogenic sources, respectively. As $\text{POC}_{\text{petro}}$ is radiocarbon-dead ($\text{Fm}_{\text{petro}} = 0$), the two equations can be combined and rearranged to yield:

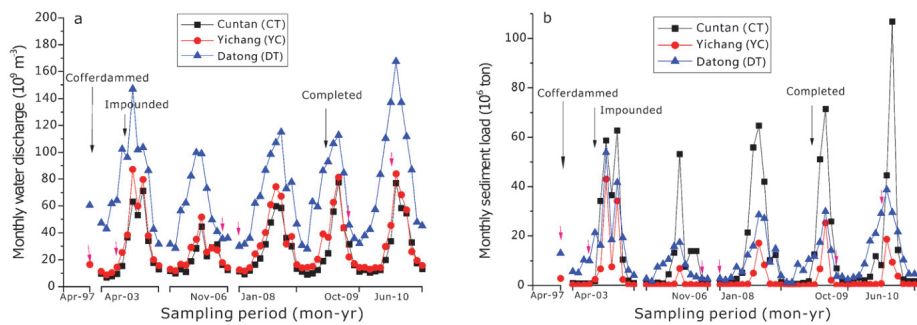


Figure 2. Variation of monthly water discharge (a) and sediment load (b) in three gauging stations in the upper (Cuntan, CT), middle (Yichang, YC), and lower (Datong, DT) reaches, during sampling periods. Except limited information available in 1997; the monthly variation of sediment load and water discharge in other years were fully presented.

$$Fm \times POC_{org} = Fm_{bio} (POC_{org} - POC_{petro}) \quad (3)$$

Thus, if a linear fit is observed between POC_{org} (X) and $Fm \times POC_{org}$ (Y), the intercept and slope of the linear correlation can be used to calculate Fm_{bio} and POC_{petro} , respectively, of the measured samples (Figure S1 and Table S3).

A three-end-member mixing model then was employed using both $\Delta^{14}C$ and $\delta^{13}C$ values to assess the relative fractional contributions of modern biomass (f_B), pre-aged soil (f_S), and ancient fossil material (f_F) to the Changjiang POC. This model can be written as follows:

$$\Delta^{14}C_{POC} = [f_B \times \Delta^{14}C_B] + [f_S \times \Delta^{14}C_S] + [f_F \times \Delta^{14}C_F] \quad (4)$$

$$\delta^{13}C_{POC} = [f_B \times \delta^{13}C_B] + [f_S \times \delta^{13}C_S] + [f_F \times \delta^{13}C_F] \quad (5)$$

$$f_B + f_S + f_F = 1 \quad (6)$$

In order to avoid errors from arbitrary assignment of end-member values, a random sampling Monte Carlo (MC) simulation strategy was implemented to assess the source variability in the end-member values (Li et al., 2012).

2.5. Statistical Analyses

In the MC simulation strategy, end-member values ($\Delta^{14}C$ and $\delta^{13}C$) are assumed to follow a normal distribution within a given mean and standard deviation. The analysis was run in MATLAB (version R2013a, MathWorks, USA). Briefly, the program was run in Enthought Python Distribititon7.2. Out of 100 million random samples from the normal distribution of each end-member, 1 million were selected simultaneously to fulfill the given system (Li et al., 2012). Based on random sampling of each parameter value for five times, the variation of the mean values for each end-member was determined to be less than 0.2%, indicating statistical stability of the model.

Statistical differences of $\Delta^{14}C$ values in depth profile samples were calculated using one-way analysis of variance. Statistically significant differences are discussed within the 95% confidence interval.

3. Results

3.1. Variation of Water Discharge and Sediment Load

The monthly data from three gauging stations on the Changjiang mainstem—Cuntan (CT) in the TGR, YC downstream of the TGD, and DT in the lower reach (Figure 2)—revealed a seasonal pattern of variability in sediment load and water discharge (Council of Changjiang Hydrology, 2003, 2006, 2008, 2009, 2010). The difference from CT to YC and YC to DT reflects material trapped in the TGR and the contribution of middle reaches. Higher sediment loads were observed in CT station, while higher water discharges were observed in DT station, especially in flood season. The decline of sediment load at YC station after 2003 is significant. Both 2006 and 2008 were drought years based on annual fluxes of water discharge and sediment load.

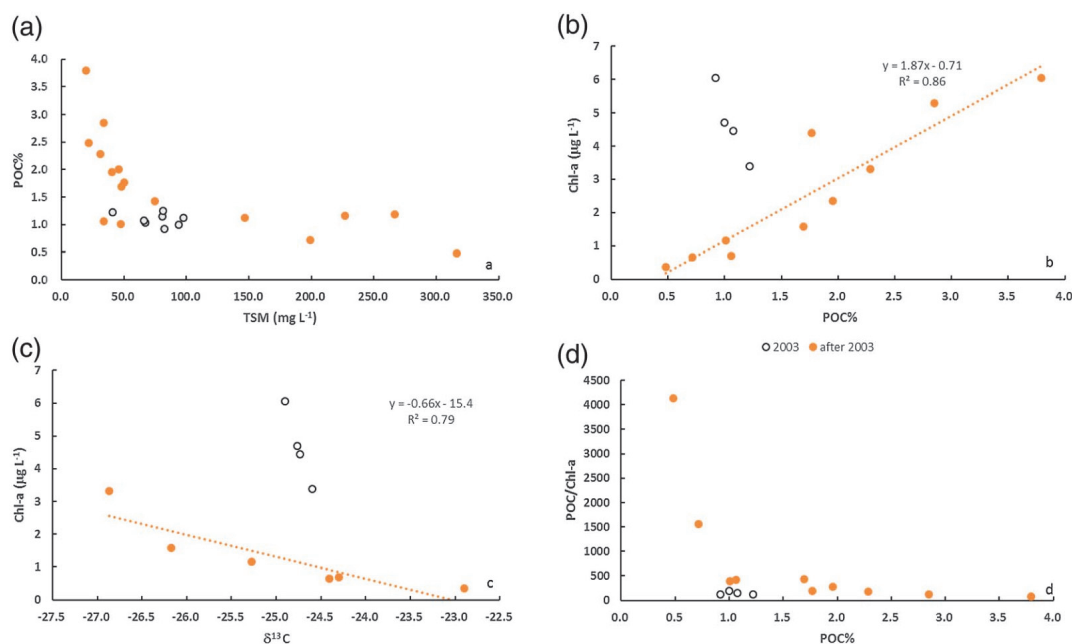


Figure 3. Relationships between organic geochemical proxies of suspended particulate matter samples of the Changjiang: (a) particulate organic carbon content (POC%) versus total suspended matter (TSM) concentration (mg/L); (b) chlorophyll-a (Chl-a) concentrations ($\mu\text{g/L}$) versus POC%; (c) Chl-a versus stable isotope composition of POC ($\delta^{13}\text{C}$, ‰); (d) ratio of POC/Chl-a versus POC%. Open symbols correspond to samples collected in 2003, and solid symbols correspond to samples collected after 2003. Regression lines in (b) and (c) are for post-2003 samples only.

Notably, the middle and lower reaches suffered from extreme storms and freezing rains during January 2008, which resulted in similar sediment loads across all three stations. The lowest water discharge values were recorded in the dry season (e.g., November and January) in the upper reach (CT and YC stations). Reservoir impoundment to water level of 175 m in September 2009 resulted in similarly low water discharge for all three stations. The highest values of water discharge were measured in the flood season of 2010. During both the impoundment of the TGR (October 2009) and the July 2010 flood season, the sediment load was highest at CT and lowest at YC, implying high trapping efficiency by TGD during these periods.

3.2. TSM Concentrations and POC Contents

Average values for general geochemical parameters (TSM, POC%, $\delta^{13}\text{C}$, and Chl-a) obtained from all the surveys are summarized in Table 1. TSM concentrations exhibited strong spatial and temporal variations. Lower values ($<50 \text{ mg/L}$) were observed in dry seasons, with elevated values in normal seasons ($\sim 60\text{--}80 \text{ mg/L}$), and the highest values (up to $200\text{--}300 \text{ mg/L}$) during the flood season. During the 2009 impoundment period, the TSM concentrations of the upper reach were as high as 283 mg/L , whereas the values in the middle and lower reaches were only $\sim 50 \text{ mg/L}$. POC contents (expressed as the percentage of POC in TSM, POC%) ranged from 0.6% to 3.8%, with higher POC contents during the dry seasons, especially in the middle reach. In both flood and normal seasons, the mean value of POC in the upper, middle, and lower reaches was $\sim 1.1\%$, with no clear spatial variation, although POC% values were inversely correlated with TSM concentrations (Figure 3a). Similarly, while there were no obvious spatial variations in POC concentration (expressed as mg/L) within the data set, POC and TSM concentrations were positively correlated ($R^2 = 0.75$).

TSM and POC% of depth profile samples did not reveal large vertical variation in either 2009 or 2010, although the average POC contents were higher in 2010 ($\sim 1.1\%$) than in 2009 ($\sim 0.7\%$; Table 2). POC% of TSM from the tributaries was much more variable, ranging from 0.9% to 10.7%, with the highest values in the southern tributaries of the middle reach. TSM concentrations varied by over an order of magnitude between 2009 and 2010 (e.g., at YC station the average TSM in 2009 was only 21.8 mg/L , whereas in 2010 it was as high as 354 mg/L), whereas the POC% showed little variation. The TSM concentrations in the upper reach during 2009 were similar to those in the upper and middle reaches in 2010. The lowest values were observed at YC

Table 2

TSM Concentrations (TSM samples only), Organic Carbon Contents (POC%), and Bulk Stable Carbon Isotope ($\delta^{13}\text{C}$, ‰) and Radiocarbon Compositions (Conventional ^{14}C Age, Years BP) of Organic Carbon in Suspended Particulate Matter and Sediments in the Changjiang Basin

Sampling period	Station	Location	Water depth (m)	TSM (mg/L)	POC (%)	$\delta^{13}\text{C}_{\text{org}}$	Conventional age (BP)	SD
Oct 2009	SG	Upper reach	0	318.4	0.3	-23.7	4,550	45
			0	317.9	0.5	-25.0	3,820	35
			1	331.7	0.5	-25.0	3,210	35
			2.5	341.8	0.5	-25.5	3,940	35
			4	327.8	0.5	-25.1	5,820	35
	JJ	Upper reach	0	443.6	0.4	-24.6	4,110	30
			2	485.7	0.4	-24.5	4,410	30
			4	476.9	0.4	-24.6	3630	55
			5.5	561.3	0.4	-24.6	5,280	50
	YC	Upper reach	0	22.7	0.8	-25.7	1,390	25
			8.5	21.1	1.2	-24.6	1,470	25
			13.5	21.5	1.0	-26.2	1,600	30
	HS	Middle reach	0	42.4	1.0	-24.9	2,670	30
			10	60.6	0.5	-24.8	4,390	30
	WU	Lower reach	0	69.0	1.0	-25.7	2,190	30
			4.5	57.3	0.9	-25.7	2,200	25
			8	61.0	0.9	-25.5	1,900	25
			13.5	55.5	0.8	-25.9	2,360	25
	XLJ	Lower reach	0	27.2	0.8	-26.0	2,090	30
			4.5	33.7	0.8	-25.4	2,350	35
			9	36.0	0.8	-25.7	2,250	25
			14.5	40.7	0.8	-25.6	2,240	25
	WJ	Tributary	0	8.4	3.2	-25.9	1,960	25
	YLJ	Tributary	0	14.0	1.3	-24.5	3,340	30
	JLJ	Tributary	0	31.0	0.9	-25.2	2,110	25
	GJ	Tributary	0	10.0	10.7	-26.2	590	25
	HJ	Tributary	0	84.8	0.9	-25.8	1,540	30
	XJ	Tributary	0	3.0	9.5	-28.5		
Aug 2010	FJ	Upper reach	0	307.1	1.3	-24.8	3,430	30
			20	374.0	1.1	-24.2		
			40	384.0	1.1	-24.5		
			60	423.0	1.1	-24.5		
			80	401.0	1.1	-24.3		
			125	363.5	1.2	-24.5		
	YC	Upper reach	0	365.2	1.0	-24.5	2,820	30
			4.5	356.2	1.1	-24.2		
			9	307.8	0.8	-24.6		
			14	353.9	1.1	-24.2		
			18	373.9	1.0	-24.4		
	CLJ	Middle reach	22	369.5	1.1	-24.6		
			0	252.8	1.2	-24.5	2,740	30
	WH	Middle reach	20	236.7	1.0	-24.7		
			0	159.7	1.2	-25.2	2,030	30
	JJ	Lower reach	18	172.0	1.2	-25.2		
			0	157.3	1.0	-25.6	1,570	30
	JY	Lower reach	18	173.7	1.2	-25.1		
			0	136.5	1.2	-25.1	2,960	30
	DTH	Tributary	0	14.8	8.9	-29.2	910	30
	HJ	Tributary	0	123.1	1.3	-24.5	2,020	30
	PYH	Tributary	0	28.6	3.2	-30.4	1,570	30

Note. TSM = total suspended matter; POC = particulate organic carbon; SD = standard deviation; BP = before present; SG = Shigu; YC = Yichang; XLJ = Xulijing; WJ = Wujiang; GJ = Ganjiang; HJ = Hanjiang; XJ = Xiangjiang; FJ = Fujiang; DTH = Dongtinghu; HJ = Hanjiang; PYH = Poyanghu; NX = Nanxi; JJ = Juijiang; HS = Huangshi; WU = Wuhu; YLJ = Yalongjiang; JLJ = Jianglingjiang; CLJ = Chenlingji; WH = Wuhan; JY = Jiangyin.

in 2009. The average TSM value in the lower reach in 2009 was ~40 mg/L, in contrast to ~150 mg/L in 2010, whereas TSM content in tributaries in 2009 and 2010 were relatively invariant, with higher values observed at Hanjiang and lower values in Ganjiang (Poyang Lake) and Xiangjiang (Dongting Lake).

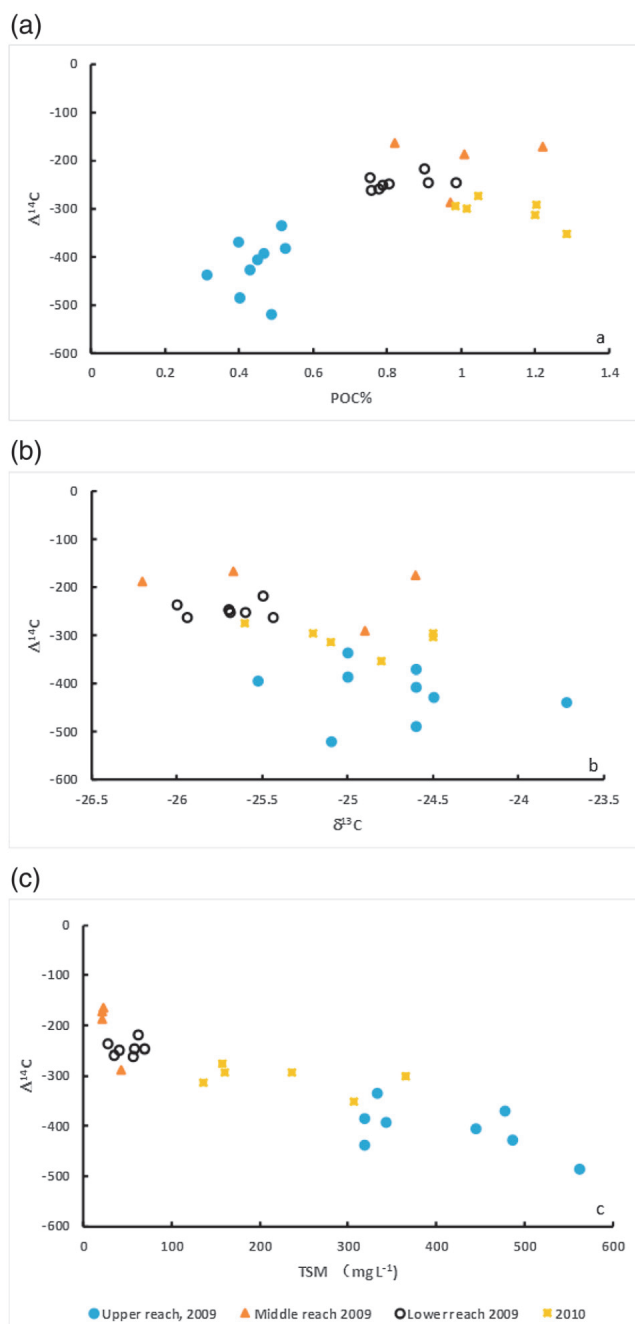


Figure 4. Relationships between radiocarbon contents of suspended particulate organic carbon (POC; $\Delta^{14}\text{C}$ values, ‰) with (a) POC%, (b) POC stable carbon isotope composition ($\delta^{13}\text{C}$, ‰), and (c) total suspended matter (TSM; mg/L) of TSM samples of the Changjiang. Different color symbols correspond to samples from the upper (blue), middle (orange), and lower (gray) reaches in 2009 and from the middle and lower (yellow) reaches in 2010.

4. Discussion

As sediment is the major carrier of riverine POM, the transport and delivery of POM in large basins is strongly controlled by the provenance and magnitude of sediment supply from different sources and by hydrodynamic processes (Dai & Liu, 2013). Thus, fluvial processes can modify the composition, structure, and age of riverine POM. In this study, we seek to better characterize the nature of POM transported by the

3.3. Chl- α Concentrations and POC $\delta^{13}\text{C}$ Values

Average POC $\delta^{13}\text{C}$ values, ranging from $-26.9\text{\textperthousand}$ to $-24\text{\textperthousand}$, showed no systematic spatial and temporal variability (Table 1). Low concentrations of Chl- α (0.4–6.1 $\mu\text{g/L}$) were generally observed in the Changjiang. Chl- α concentrations and POC% exhibited a linear correlation ($R^2 = 0.86$), with the exception of data collected in April 2003 (higher values of Chl- α observed in 2003 were related to seasonal variation; Figure 3b). A similar linear relationship also exists between Chl- α and $\delta^{13}\text{C}$ (Figure 3c). The POC/Chl- α ratios varied in the range of 80–4,200, with the highest ratio observed in October 2009. The POC/Chl- α ratios were inversely correlated with POC% (Figure 3d).

POC $\delta^{13}\text{C}$ values ranged from $-26.2\text{\textperthousand}$ to $-23.7\text{\textperthousand}$ in 2009 and from $-25.6\text{\textperthousand}$ to $-24.2\text{\textperthousand}$ in 2010 (Table 2). The lowest $\delta^{13}\text{C}$ values in suspended POC were observed in the southern tributaries ($-28.5\text{\textperthousand}$ to $-30.4\text{\textperthousand}$), which are also characterized by higher POC contents (POC% values). The $\delta^{13}\text{C}_{\text{POC}}$ values of the most upstream samples from the upper reach (e.g., Shigu, $-23.7\text{\textperthousand}$) were quite close to those measured for the erosion products of Himalayan rocks (-23 to $-21\text{\textperthousand}$; Galy et al., 2007). No systematic trend in $\delta^{13}\text{C}$ values with sampling depth or spatial variation was observed in TSM samples from either the 2009 or 2010 campaigns.

3.4. POC $\Delta^{14}\text{C}$ Values

Within the depth profiles, the $\Delta^{14}\text{C}_{\text{POC}}$ values in 2009 varied between $-160\text{\textperthousand}$ and $-450\text{\textperthousand}$, corresponding to conventional ^{14}C ages of 1,600 to 4,550 years before present (BP; Figure 4 and Table 2). No systematic variations in $\Delta^{14}\text{C}$ values with depth were evident ($p > 0.4$), but samples from bottom layers tended to be lower at most stations. The $\Delta^{14}\text{C}$ values of surface POC in 2010 were more uniform, varying from $-270\text{\textperthousand}$ to $-350\text{\textperthousand}$ (mean ^{14}C age, 2,500 years BP). The $\Delta^{14}\text{C}_{\text{POC}}$ values for tributaries in both 2009 and 2010 were higher (younger) compared to those for mainstem samples, especially for the tributaries of the middle reach (mean ^{14}C age 1,500 years BP), indicating fresher POM.

There is a nonlinear positive correlation between POC $\Delta^{14}\text{C}$ and POC% values in samples from the 2009 survey (Figure 4a), with higher POC contents generally corresponding with higher $\Delta^{14}\text{C}$ values (younger ^{14}C ages). The youngest ^{14}C ages were measured immediately below the TGD (YC) in 2009. However, values for the 2010 survey samples do not exhibit the same relationship (Figure 4a).

A cross-plot of POC $\delta^{13}\text{C}$ versus $\Delta^{14}\text{C}$ values indicates a general relationship in the Changjiang basin whereby relatively low ^{13}C values correspond to higher $\Delta^{14}\text{C}$ values (younger ^{14}C ages), and vice versa (Figure 4b). A strong linear relationship is evident between $\Delta^{14}\text{C}_{\text{POC}}$ and TSM in the overall data set ($R^2 = 0.81$), with lower TSM concentrations corresponding with higher $\Delta^{14}\text{C}$ values (younger ^{14}C ages; Figure 4c).

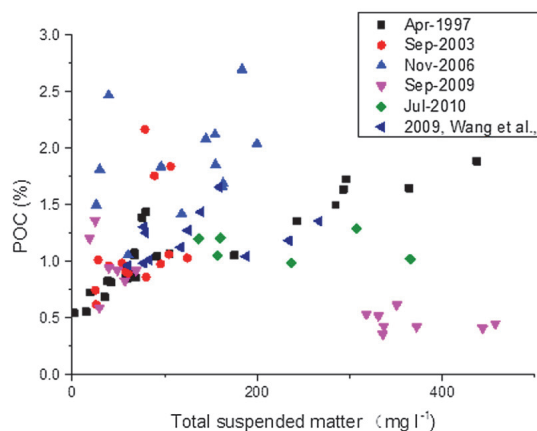


Figure 5. Relationships between particulate organic carbon (POC%) and total suspended matter based on series observations and literature data.

$1.86\% \pm 0.8\%$) than in the upper and lower reaches (average $1.10\% \pm 0.3\%$), especially during the dry season. This may reflect contributions from two lake systems in the middle reach that have extremely high POC% values ($>4\%$) compared with other tributaries. However, corresponding $\delta^{13}\text{C}$ values do not indicate additional sources of POM in the middle reach. Considering the decline of sediment load within the basin as a consequence of the TGD, we expect that the accompanying decrease of TSM may promote in situ production and hence an increase in POC%. This interpretation is supported by the lower TSM concentrations observed in the dry season corresponding to higher POC% values and by the correlation between Chl- α and POC% in samples collected subsequent to 2003 (Figure 3 and Table 2). The TSM ratio (ratio of the average TSM values of the lower versus middle reach, or the middle versus upper reach) exhibits a clear linear correlation with the sediment-load ratio (using the sediment loads of CT, YC, and DT to represent the upper, middle, and lower reaches, respectively; $r^2 = 0.95$ if data collected during extreme weather in January 2008 are excluded, and $r^2 = 0.66$ if including all data; Figure 6a). The POC% ratio (between various sub-basins) also exhibits a negative correlation with the sediment-load ratio (between various sub-basins), and while this correlation is weaker ($r^2 = 0.82$, excluding data collected during the impoundment period in September 2009), it suggests that dilution of TSM is a major process controlling POC content of TSM in the Changjiang watershed (Figure 6b). High POC/Chl- α ratios indicate that POM is dominated by detritus (high values of >200 ; Figure 3d), although an autochthonous contribution is also likely present (Bao et al., 2015). The contrasting behavior between

Changjiang and its tributaries and to assess potential temporal variations in response to seasonal, interannual, and anthropogenic influences.

4.1. Spatiotemporal Variations in POC Transported by the Changjiang

Several prior studies have examined the origin, composition, transport, and flux of OM in the Changjiang basin. The TSM and POC% values measured in this study are comparable to those of previous studies (Bao et al., 2015; Wang et al., 2012; Wu et al., 2007, 2015; Yu et al., 2011; Zhang et al., 2014) (Table 2 and Figure 5). Before the operation of TGD (2003), TSM concentration and POC% exhibited a positive correlation and spanned a lower range of POC% values (less than 2%). After 2003, the variability in POC% values became greater, with higher values of POC% frequently observed in low TSM samples. As suggested previously, soil OM represents the major source for POM in this basin, which could explain lower POC% observed in this system (Wu et al., 2007). Our results suggest that POC% values in the middle reach are higher (average

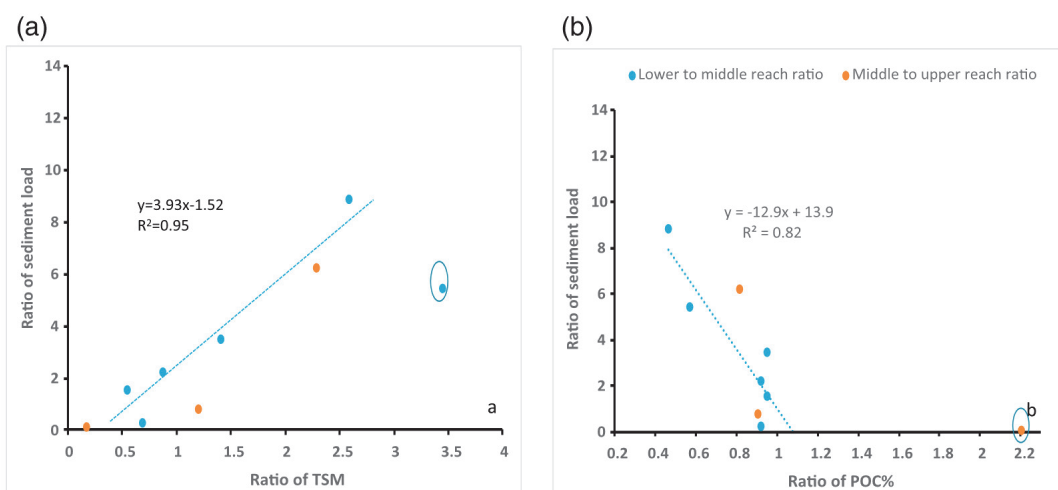


Figure 6. Relationships between (a) ratio of total suspended matter (TSM) versus ratio of sediment load and (b) ratio of POC% versus ratio of sediment load among sub-basins of the Changjiang, the ratio of middle-to-upper reach (represented as orange symbols) and the ratio of lower-to-middle reach (represented as blue symbols).

Table 3
Estimation of Biospheric Organic Carbon Fm Values and Petrogenic Carbon Contents (wt%) Based on a Two-End-Member Mixing Model

Sample	Period	Depth (m)	POC (wt%)	POC _{petro} (wt%)	Fm _{bio}	
SG (upper reach)	Oct 2009	0	0.31	0.11	0.46	
		Bedload	0.09			
NX (upper reach)		0	0.52	0.13	$0.87 \pm 0.03 (r^2 = 0.81)$	
		1	0.51			
		2.5	0.46			
		0	0.82			
YC (upper reach)		8.5	1.22	0.02	$0.82 \pm 0.07 (r^2 = 0.99)$	
		13.5	1.01			
		0	0.97			
		10	0.52			
HS (middle reach)		Bedload	0.08	0.08	$0.76 \pm 0.01 (r^2 = 0.99)$	
		0	0.98			
		4.5	0.91			
		8	0.90			
WU (lower reach)		13.5	0.75	0.07	$0.83 \pm 0.02 (r^2 = 0.98)$	
		0	0.75			
		4.5	0.78			
		9	0.78			
Upper tributaries				0.14	$0.81 \pm 0.04 (r^2 = 0.99)$	
Middle and lower tributaries				0.11	$0.94 \pm 0.02 (r^2 = 0.99)$	
TGD region	Aug 2010			0.22	$0.67 \pm 0.02 (r^2 = 0.99)$	
Middle stream				0.01	$0.72 \pm 0.02 (r^2 = 0.99)$	
Lower stream				0.13		
Middle and lower tributaries				0.26	$0.75 \pm 0.02 (r^2 = 0.99)$	
Whole basin	Oct 2009			0.09	$0.83 \pm 0.04 (r^2 = 0.99)$	
Whole basin	Aug 2010			0.06	$0.79 \pm 0.02 (r^2 = 0.99)$	

Note. POC = particulate organic carbon; SG = Shigu; YC = Yichang; XLJ = Xulujing; TGD = Three Gorges Dam; NX = Nanxi; HS = Huangshi; WU = Wuhu.

Chl- α versus POC% and $\delta^{13}\text{C}$ subsequent to 2003 suggests that the construction of the TGD resulted in enhanced contributions from autochthonous OM to POC in the middle and lower reaches of the river (Figure 3).

4.2. Appportionment of POC Sources in the Changjiang Basin

Riverine POC consists of three primary inputs: recently synthesized biomass and detritus from terrestrial and/or aquatic primary producers, pre-aged soil OM, and fossil material (Goñi et al., 2005; Marwick et al., 2015; Tao et al., 2015). Here we apply two approaches to constrain the contributions of different sources: a dual-isotopic mass balance (Drenzek et al., 2007) and a binary mixing model based on bulk ^{14}C compositions (Galy et al., 2008; Galy & Eglinton, 2011).

The binary mixing analysis results for the Changjiang samples are summarized in Table 3. With the exception of the uppermost station in 2009, most suspended particles in the Changjiang River are dominated by POC_{bio} (~60–80% of total POC). Higher Fm_{bio} values observed for the tributaries may be related to higher in situ production in those areas due to eutrophication. Lower Fm_{bio} values were found for samples collected in the TGD region during the flood season of 2010 and imply trapping of fossil material in the upper reach. Corresponding estimates for the average POC_{bio} ^{14}C age of these samples varied from ~1,500 years in October 2009 to ~2,000 years in August 2010. These values are close to estimates of POC_{bio} age from the Amazon River (1,120–2,750 years; Bouchez et al., 2014) and the Ganges River (1,600–2,960 years; Galy & Eglinton, 2011) but younger than the values for the Yellow River (3,190–4,790 years; Tao et al., 2015) and the Mackenzie River (3,030–7,900 years; Hilton et al., 2015). Since the binary mixing model is based on a linear fit of available data, its robustness is dependent on sample density. Furthermore, depth profile $\Delta^{14}\text{C}$ data are not available for 2010; we only could make a rough estimation of the origin of OM from different regions

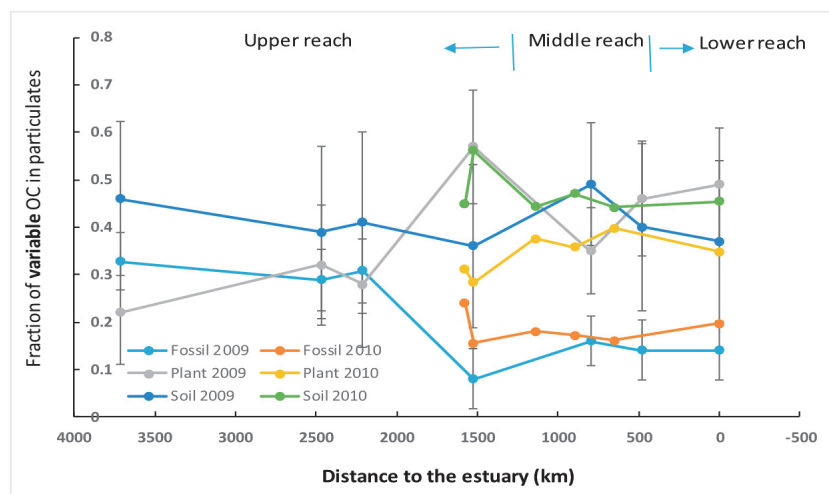


Figure 7. Results from model calculations for mean proportions of modern biomass (orange symbols), pre-aged soil (gray symbols), and fossil organic carbon (OC; blue symbols) in the Changjiang; error bar was illustrated for each point based on model calculations.

(Table 3). More detailed sampling would be necessary to further constrain POC sources. Moreover, since POC versus $\delta^{13}\text{C}$ suggests that soil OM represents the major sources of riverine POC, it is important to separately assess contributions of pre-aged soil OC.

For the three end-member mixing model, we assign different end-members for fossil biomass, modern biomass, and pre-aged soil for the upper reach and for the middle and lower reaches in order to reflect regional variability in end-members (e.g., variable $\delta^{13}\text{C}$ values of plants and fossil material; Yu et al., 2007). In particular, because of the high trapping efficiency of the TGR after its emplacement in 2003 (Yang et al., 2015), the contribution of sediment from the upper reach to the middle and lower reaches declined significantly. The fossil material end-member of the upper reach exhibits typical characteristics of Himalayan rock ($\delta^{13}\text{C}$ and $\Delta^{14}\text{C}$ values of $-20.3\text{‰} \pm 1.5\text{‰}$ and $-950\text{‰} \pm 50\text{‰}$, respectively; Galy et al., 2008). The values of higher plants are assigned to be $\delta^{13}\text{C} = -31.7\text{‰} \pm 2\text{‰}$ for the upper reach and $\delta^{13}\text{C} = -28.5\text{‰} \pm 2\text{‰}$ for the middle and lower reaches, with $\Delta^{14}\text{C} = 0\text{‰} \pm 50\text{‰}$ for both regions (Yu et al., 2007). The end-member compositions of soil assignments are difficult to infer, especially with respect to $\Delta^{14}\text{C}$ values given that the soil OM could derive from different soil depths. We use the average values of various soil samples (top 10 cm; $n = 7$) collected from the whole basin as the end-member ($-276\text{‰} \pm 30\text{‰}$) and an average $\delta^{13}\text{C}$ value of $-23.0\text{‰} \pm 2\text{‰}$. Figure 7 shows results of the model calculations for mean proportions of modern biomass, pre-aged soil, and fossil OC in the Changjiang for 2009 and 2010. The MC simulations yield standard deviations in model calculations of 5% to 7% for fossil material, 9%–15% for modern biomass, and 17%–56% for pre-aged soil. We calculate average proportions for Changjiang suspended OC load of 38% ($\pm 13\%$) modern labile OC, 41% ($\pm 18\%$) pre-aged soil OC, and 21% ($\pm 6\%$) fossil OC in 2009. Corresponding values for 2010 were 35% ($\pm 15\%$), 47% ($\pm 21\%$), and 18% ($\pm 7\%$), respectively. Estimates for the fraction of fossil OC in the upper reach are as high as 30%, which is similar to the proportion of fossil material in the Yellow River but which contains higher pre-aged soil OC (Tao et al., 2015). Higher proportions of fossil OC and lower proportions of modern labile OC are observed in the middle and lower reaches in 2010 compared with 2009 (Figure 7), whereas there is only a minor difference in the fraction of pre-aged soil OC. Similar behavior was also observed in the Mississippi/Atchafalaya River (Rosenheim et al., 2013). Differences in POC ^{14}C age during high and low discharge periods in the Changjiang were limited (Figure 4), similar to observations for other large passive margin river systems (Blair & Aller, 2012; Rosenheim et al., 2013; Rosenheim & Galy, 2012). Our results show that the Changjiang suspended load is composed of a mixture of POC, and that variable contributions of pre-aged soil may exert a strong influence on POC ^{14}C age.

The estimated contribution of fossil material is lower in the three-end-member model compared to the two-end-member model. This difference between the two models may reflect insufficient data density to fully constrain the two-end-member model, as also noted in a study of the Yellow River (Tao et al., 2015). But

the binary analysis results rely on distinctive end-member compositions and are easy to compare with other river systems directly, while the three-end-member model quite depends on the reliability of end-member compositions for better estimations. However, both models return higher values for the proportion of fossil OC in the Changjiang TSM (0.07–0.13%) relative to other river systems (0.02–0.06%) such as the Amazon, Ganges-Brahmaputra, and Yellow Rivers (Bouchez et al., 2014; Galy et al., 2008; Tao et al., 2015) but lower than those reported in a previous study of the Changjiang that used estimates derived from a station within an urban setting (Nanjing) in the middle reach ($0.46\% \pm 0.1\%$; Li et al., 2015). The estimated contribution of modern biomass is also lower in the three-end-member model, underlining the significance of pre-aged soil OM.

4.3. Interannual Variability in POC and the Impact of the TGD

Our findings are generally consistent with previous studies indicating that large passive margin rivers deliver a minor component of fossil (petrogenic and fossil fuel) OC, with the majority derived from contemporary and pre-aged soil biospheric OC (Blair & Aller, 2012). This suggests that such river basins can be regarded as large-scale processing systems whereby hydrodynamic and remineralization processes modify the original POM signal during transport. The spatial and temporal variations in POM ages, which are similar to those previously reported for this river system (Li et al., 2015; Wang et al., 2012), result from a complicated interplay between geological, hydrological, and biogeochemical processes operating throughout the entire basin. Coupled ramped pyrolysis and ^{14}C analysis of Mississippi River POM revealed that while older POC occurred during higher discharge, no single component of the POC is responsible for the increased age (Rosenheim et al., 2013). This compositional complexity is potentially resulted from in situ reworking and exchange within the floodplain (Blair & Aller, 2012). The linear relationship between TSM and $\Delta^{14}\text{C}$ (Figure 4c) suggests that TSM sampled in the middle and lower reaches in 2010 reflects a binary mixture of contributions from upper and lower regions. This observation, together with the apparent linear relationship between the TSM ratio of the upper to middle reaches (based on the average values listed in Table 1) and the sediment-load ratio ($r^2 = 0.95$), reveals a consistent pattern of progressively older riverine POC age with increasing suspended sediment load, as has also been observed in a global compilation of river data (Marwick et al., 2015). Depleted $\Delta^{14}\text{C}$ values observed in the middle and lower reaches in 2010 reflect contributions from the upper reach during higher discharge. The impoundment in the TGR in 2009 rendered the relationship between $\Delta^{14}\text{C}$ and TSM discontinuous in basin scale. $\Delta^{14}\text{C}$ values at YC in 2009 are slightly higher ($-203\text{‰} \pm 30\text{‰}$) than those of lower reach ($-282\text{‰} \pm 75\text{‰}$), indicating an accumulation of fresher OC in the TGR. This finding is consistent with a recent study of pCO_2 dynamics in the reservoir, which indicates that TGR exerts an important influence that has altered OM composition and bioavailability in the middle and lower reaches (Liu et al., 2016). The somewhat lower and more constant $\Delta^{14}\text{C}$ values at the lower reach could reflect channel erosion and sediment resuspension processes in the middle and lower reaches (Dai & Liu, 2013).

Based on annual fluxes derived from sediment trapped within the TGR (Hu et al., 2009) as well as our POC data collected in YC, we estimate a POC burial flux in the TGD of $\sim 1.63\text{-Mt POC/year}$ since 2003. This burial flux is lower than that obtained in a previous study ($\sim 2.1\text{-Mt POC/year}$; Li et al., 2015). For comparison, the POC export flux for 2003–2014 from the Changjiang, estimated from the sediment load at DT (lower reach), was 0.87- to 2.77-Mt POC/year (average $\sim 1.78\text{-Mt POC/year}$; Wu et al., 2015). These estimates demonstrate that the TGD plays an important role in trapping POM from the upper reaches of the Changjiang. A recent study of CO_2 fluxes from the TGR concluded that CO_2 emissions are only about 0.17 Mt/year during the high-water-level period (Fu et al., 2016), implying that the TGR is an efficient carbon sink. Continuous monitoring of CO_2 degassing from the Changjiang estuary indicates that this area acts as a moderate or significant sink of atmospheric CO_2 in winter, spring, and summer and only becomes a net CO_2 source in autumn (Zhai & Dai, 2009). This implies an increase in delivery of fresh OC to the East China Sea (ECS) shelf, potentially leading in the future to the ECS shifting from serving as a sink to a source for atmospheric CO_2 . The operation of the TGD is thus modifying the source, composition, and ages of POM in the Changjiang, especially in middle and lower reaches, with accompanying changes in the regional carbon balance. Specific changes include accelerated POC accumulation in the TGR, higher primary production in middle-lower reaches, and delivery of fresher OC to ECS, potentially modifying the role of the ECS in regulating atmospheric CO_2 . Sustained observations and modeling for assessment of ongoing change, as well as prediction of future changes in the Changjiang-ECS system—and indeed other anthropogenic impacted large rivers—is therefore important for assessment of regional- and global-scale impacts.

5. Conclusions

In this study, we report a comprehensive data set that reveals spatial and temporal variations in POM ages and characteristics throughout the Changjiang basin. Dual-carbon isotopic mixing models suggest that three primary sources of OM contribute to the modern-day (2009 and 2010) Changjiang suspended load: modern biomass OC from fresh higher plant detritus and aquatic production, pre-aged soil OM, and fossil (petrogenic) OC. A higher fraction of fossil OC and lower fraction of modern labile OC were observed in the middle and lower reaches in 2010 compared with 2009. From a two-end-member mixing model, we estimate that average ^{14}C ages derived from Fm_{bio} were $\sim 1,500$ and $\sim 2,000$ years for 2009 and 2010, respectively, comparable to similarly derived ^{14}C ages for the Amazon and Ganges TSM but younger than Yellow River TSM. Both mixing models suggest that soil OC comprises the major component of Changjiang POC. Since its completion in 2003, the TGD has resulted in trapping a significant portion of POC behind the dam. POM in the middle and lower reaches has correspondingly shifted to younger, fresher material, with potentially broad implications for biogeochemical processes throughout the Changjiang-ECS system. Further investigations are necessary to assess impacts of the decline in sediment load and associated decrease of the supply of refractory fossil carbon from large river systems on carbon budgets in adjacent marginal seas.

Acknowledgments

Data supporting Figures 2, 4, 6, and 7 are available as in supporting information Tables S2–S4. This study was funded by the Natural Science Foundation of China (41530960 and 41276081). The authors thank all colleagues in the Marine Biogeochemistry group in SKLEC for their assistance with the field and laboratory work. W. Y. acknowledges the staff of NOSAMS for their support for ^{14}C analysis. The authors thank for the comments and suggestions from all the reviewers.

References

Aufdenkampe, A. K., Mayorga, E., Raymond, P. A., Melack, J. M., Doney, S. C., Alin, S. R., et al. (2011). Riverine coupling of biogeochemical cycles between land, oceans, and atmosphere. *Frontiers in Ecology and the Environment*, 9(1), 53–60. <https://doi.org/10.1890/100014>

Bao, H., Wu, Y., & Zhang, J. (2015). Spatial and temporal variation of dissolved organic matter in the Changjiang: Fluvial transport and flux estimation. *Journal of Geophysical Research: Biogeosciences*, 120, 1870–1886. <https://doi.org/10.1002/2015JG002948>

Battin, T. J., Luyssaert, S., Kaplan, L. A., Aufdenkampe, A. K., Richter, A., & Tranvik, L. J. (2009). The boundless carbon cycle. *Nature Geoscience*, 2(9), 598–600. <https://doi.org/10.1038/ngeo618>

Benner, R. (2004). What happens to terrestrial organic matter in the ocean? *Marine Chemistry*, 92(1–4), 307–310. <https://doi.org/10.1016/j.marchem.2004.06.033>

Bianchi, T. S., & Allison, M. A. (2009). Large-river delta-front estuaries as natural “recorders” of global environmental change. *Proceedings of the National Academy of Sciences*, 106(20), 8085–8092. <https://doi.org/10.1073/pnas.0812878106>

Blair, N. E., & Aller, R. C. (2012). The fate of terrestrial organic carbon in the marine environment. *Annual Review of Marine Science*, 4(1), 401–423. <https://doi.org/10.1146/annurev-marine-120709-142717>

Borges, A. V., Darchambeau, F., Teodoru, C. R., Marwick, T. R., Tamoh, F., Geeraert, N., et al. (2015). Globally significant greenhouse-gas emissions from African inland waters. *Nature Geoscience*, 8(8), 637–642. <https://doi.org/10.1038/ngeo2486>

Bouchez, J., Galy, V., Hilton, R. G., Gaillardet, J., Moreira-Turcq, P., Pérez, M. A., & Maurice, L. (2014). Source, transport and fluxes of Amazon River particulate organic carbon: Insights from river sediment depth-profiles. *Geochimica et Cosmochimica Acta*, 133, 280–298. <https://doi.org/10.1016/j.gca.2014.02.032>

Council of Changjiang Hydrology (2003). *Changjiang Sediment Bulletin* [in Chinese] (pp 24). Press of Changjiang, Beijing.

Council of Changjiang Hydrology (2006). *Changjiang Sediment Bulletin* [in Chinese] (pp. 34). Press of Changjiang, Beijing.

Council of Changjiang Hydrology (2008). *Changjiang Sediment Bulletin* [in Chinese] (pp. 41). Press of Changjiang, Beijing.

Council of Changjiang Hydrology (2009). *Changjiang Sediment Bulletin* [in Chinese] (pp. 42). Press of Changjiang, Beijing.

Council of Changjiang Hydrology (2010). *Changjiang Sediment Bulletin* [in Chinese] (pp. 52). Press of Changjiang, Beijing.

Dai, Z., Liu, J. T., Wei, W., & Chen, J. (2014). Detection of the Three Gorges Dam influence on the Changjiang (Yangtze River) submerged delta. *Scientific Reports*, 4, 6600.

Dai, Z. J., & Liu, J. T. (2013). Impacts of large dams on downstream fluvial sedimentation: An example of the Three Gorges Dam (TGD) on the Changjiang (Yangtze River). *Journal of Hydrology*, 480, 10–18. <https://doi.org/10.1016/j.jhydrol.2012.12.003>

Drenzek, N. J., Montluçon, D. B., Yunker, M. B., Macdonald, R. W., & Eglinton, T. I. (2007). Constraints on the origin of sedimentary organic carbon in the Beaufort Sea from coupled molecular ^{13}C and ^{14}C measurements. *Marine Chemistry*, 103(1–2), 146–162. <https://doi.org/10.1016/j.marchem.2006.06.017>

Eglinton, T. I., & Eglinton, G. (2008). Molecular proxies for paleoclimatology. *Earth and Planetary Science Letters*, 275(1–2), 1–16. <https://doi.org/10.1016/j.epsl.2008.07.012>

Feng, X., Vonk, J. E., van Dongen, B. E., Gustafsson, Ö., Semiletov, I. P., Dudarev, O. V., et al. (2013). Differential mobilization of terrestrial carbon pools in Eurasian Arctic river basins. *Proceedings of the National Academy of Sciences*, 110(35), 14,168–14,173. <https://doi.org/10.1073/pnas.1307031110>

Fu, J., Gao, M., Deng, B., Zhou, Z. R., Chen, Y., Dang, C., et al. (2016). Partial pressure and diffusion flux of dissolved carbon dioxide in typical mainstream and tributaries of the Three Gorges Reservoir during high water level period (in Chinese with English abstract). *Earth & Environment*, 44, 64–72.

Galy, V., Beyssac, O., France-Lanord, C., & Eglinton, T. (2008). Recycling of graphite during Himalayan erosion: A geological stabilization of carbon in the crust. *Science*, 322(5903), 943–945. <https://doi.org/10.1126/science.1161408>

Galy, V., & Eglinton, T. (2011). Protracted storage of biospheric carbon in the Ganges-Brahmaputra basin. *Nature Geoscience*, 4(12), 843–847. <https://doi.org/10.1038/ngeo1293>

Galy, V., France-Lanord, C., Beyssac, O., Faure, P., Kudrass, H., & Palhol, F. (2007). Efficient carbon burial in the Bengal fan sustained by the Himalayan erosional system. *Nature*, 450, 407–410.

Goñi, M. A., Ruttenberg, K. C., & Eglinton, T. I. (1997). Source and contribution of terrigenous organic carbon to surface sediments in the Gulf of Mexico. *Nature*, 389(6648), 275–278. <https://doi.org/10.1038/38477>

Goñi, M. A., Ruttenberg, K. C., & Eglinton, T. I. (1998). A reassessment of the sources and importance of land-derived organic matter in surface sediments from the Gulf of Mexico. *Geochimica et Cosmochimica Acta*, 62(18), 3055–3075. [https://doi.org/10.1016/S0016-7037\(98\)00217-8](https://doi.org/10.1016/S0016-7037(98)00217-8)

Goñi, M. A., Yunker, M. B., Macdonald, R. W., & Eglinton, T. I. (2005). The supply and preservation of ancient and modern components of organic carbon in the Canadian Beaufort Shelf of the Arctic Ocean. *Marine Chemistry*, 93(1), 53–73.

Gustafsson, O., van Donden, B. E., Vonk, J. E., Dudarev, O. V., & Semiletov, L. P. (2011). Widespread release of old carbon across the Siberian Arctic echoed by its large rivers. *Biogeosciences*, 8(6), 1737–1743. <https://doi.org/10.5194/bg-8-1737-2011>

Hedges, J. I., Keil, R. G., & Benner, R. (1997). What happens to terrestrial organic matter in the ocean? *Organic Geochemistry*, 27(5–6), 195–212.

Hilton, R. G., Galy, V., Gaillardet, J., Dellinger, M., Bryant, C., O'Regan, M., & Calmels, D. (2015). Erosion of organic carbon in the Arctic as a geological carbon dioxide sink. *Nature*, 524(7563), 84–87. <https://doi.org/10.1038/nature14653>

Hu, B. Q., Yang, Z. S., Wang, H. J., Sun, X. X., Bi, N. S., & Li, G. G. (2009). Sedimentation in the Three Gorges Dam and the future trend of Changjiang (Yangtze River) sediment flux to the sea. *Hydrology and Earth System Sciences*, 13(11), 2253–2264.

Leithold, E. L., Blair, N. E., & Perkey, D. W. (2006). Geomorphologic controls on the age of particulate organic carbon from small mountainous and upland rivers. *Global Biogeochemical Cycles*, 20, GB3022. <https://doi.org/10.1029/2005GB002677>

Li, G., Wang, X. T., Yang, Z., Mao, C., West, A. J., & Ji, J. (2015). Dam-triggered organic carbon sequestration makes the Changjiang (Yangtze) river basin (China) a significant carbon sink. *Journal of Geophysical Research: Biogeosciences*, 120, 39–53. <https://doi.org/10.1002/2014JG002646>

Li, X., Bianchi, T. S., Allison, M. A., Chapman, P., Mitra, S., Zhang, Z., & Yu, Z. (2012). Composition, abundance and age of total organic carbon in surface sediments from the inner shelf of the East China Sea. *Marine Chemistry*, 145, 37–52.

Liu, S., Lu, X. X., Xia, X., Zhang, S., Ran, L., Yang, X., & Liu, T. (2016). Dynamic biogeochemical controls on river pCO₂ and recent changes under aggravating river impoundment: An example of the subtropical Yangtze River. *Global Biogeochemical Cycles*, 30, 880–897. <https://doi.org/10.1002/2016GB005388>

Longworth, B. E., Petsch, S. T., Raymond, P. A., & Bauer, J. E. (2007). Linking lithology and land use to sources of dissolved and particulate organic matter in headwaters of a temperate, passive-margin river system. *Geochimica et Cosmochimica Acta*, 71(17), 4233–4250. <https://doi.org/10.1016/j.gca.2007.06.056>

Lorenzen, C. J. (1967). Determination of chlorophyll and phaeopigments: Spectrophotometric equations. *Limnology and Oceanography*, 12(2), 343–346. <https://doi.org/10.4319/lo.1967.12.2.0343>

Marwick, T. R., Tamoh, F., Teodoru, C. R., Borges, A. V., Darchambeau, F., & Bouillon, S. (2015). The age of river-transported carbon: A global perspective. *Global Biogeochemical Cycles*, 29, 122–137. <https://doi.org/10.1002/2014GB004911>

Moreira-Turcq, P., Bonnet, M. P., Amorim, M., Bernardes, M., Lagane, C., Maurice, L., & Seyler, P. (2013). Seasonal variability in concentration, composition, age, and fluxes of particulate organic carbon exchanged between the floodplain and Amazon River. *Global Biogeochemical Cycles*, 27, 119–130. <https://doi.org/10.1002/gbc.20022>

Raymond, P. A., Bauer, J. E., Caraco, N. F., Cole, J. J., Longworth, B., & Petsch, S. T. (2004). Controls on the variability of organic matter and dissolved inorganic carbon ages in northeast US rivers. *Marine Chemistry*, 92(1–4), 353–366. <https://doi.org/10.1016/j.marchem.2004.06.036>

Rosenheim, B. E., & Galy, V. (2012). Direct measurement of terrigenous carbon age structure. *Geophysical Research Letters*, 39, L19703.

Rosenheim, B. E., Roe, K. M., Roberts, B. J., Kolker, A. S., Allison, M. A., & Johannesson, K. H. (2013). River discharge influences on particulate organic carbon age structure in the Mississippi/Atchafalaya River system. *Global Biogeochemical Cycles*, 27, 154–166. <https://doi.org/10.1002/gbc.20018>

Schefuss, E., Eglinton, T. I., Spencer-Jones, C. L., Rullkötter, J., De Pol-Holz, R., Talbot, H. M., & Schneider, R. R. (2016). Hydrologic control of carbon cycling and aged carbon discharge in the Congo River basin. *Nature Geoscience*, 9(9), 687–690. <https://doi.org/10.1038/ngeo2778>

Tao, S. Q., Eglinton, T. I., Montlucou, D. B., McIntyre, C., & Zhao, M. X. (2015). Pre-aged soil organic carbon as a major component of the Yellow River suspended load: Regional significance and global relevance. *Earth and Planetary Science Letters*, 414, 77–86. <https://doi.org/10.1016/j.epsl.2015.01.004>

Tranvik, L. J., Downing, J. A., Cotner, J. B., Loiselle, S. A., Striegl, R. G., Ballatore, T. J., & Kortelainen, P. L. (2009). Lakes and reservoirs as regulators of carbon cycling and climate. *Limnology and Oceanography*, 54(6part2), 2298–2314. https://doi.org/10.4319/lo.2009.54.6_part_2.2298

Wang, X., Ma, H., Li, R., Song, Z., & Wu, J. (2012). Seasonal fluxes and source variation of organic carbon transported by two major Chinese rivers: The Yellow River and Changjiang (Yangtze) River. *Global Biogeochemical Cycles*, 26, GB2025. <https://doi.org/10.1029/2011GB004130>

Wu, Y., Bao, H., Yu, H., Zhang, J., & Kattner, G. (2015). Temporal variability of particulate organic carbon in the lower Changjiang (Yangtze River) in the post-Three Gorges Dam period: Links to anthropogenic and climate impacts. *Journal of Geophysical Research: Biogeosciences*, 120, 2194–2211. <https://doi.org/10.1002/2015JG002927>

Wu, Y., Zhang, J., Liu, S. M., Zhang, Z. F., Yao, Q. Z., Hong, G. H., & Cooper, L. (2007). Sources and distribution of carbon within the Yangtze River system. *Estuarine, Coastal and Shelf Science*, 71(1–2), 13–25. <https://doi.org/10.1016/j.ecss.2006.08.016>

Yang, S. L., Li, M., Dai, S. B., Liu, Z., Zhang, J., & Ding, P. X. (2006). Drastic decrease in sediment supply from the Yangtze River and its challenge to coastal wetland management. *Geophysical Research Letters*, 33, L06408. <https://doi.org/10.1029/2005GL025507>

Yang, S. L., Milliman, J. D., Li, P., & Xu, K. (2011). 50,000 dams later: Erosion of the Yangtze River and its delta. *Global and Planetary Change*, 75(1–2), 14–20. <https://doi.org/10.1016/j.gloplacha.2010.09.006>

Yang, S. L., Xu, K. H., Milliman, J. D., Yang, H. F., & Wu, C. S. (2015). Decline of Yangtze River water and sediment discharge: Impact from natural and anthropogenic changes. *Scientific Reports*, 5(1), 12581. <https://doi.org/10.1038/srep12581>

Yu, H., Wu, Y., Zhang, J., Deng, B., & Zhu, Z. (2011). Impact of extreme drought and the Three Gorges Dam on transport of particulate terrestrial organic carbon in the Changjiang (Yangtze) River. *Journal of Geophysical Research*, 116, F4029. <https://doi.org/10.1029/2011JF002012>

Yu, H., Wu, Y., Zhang, J., Yao, Q. Z., & Zhu, Z. Y. (2007). The characteristics of lignin of plants and soil samples in the Yangtze River (Changjiang) drainage basin (in Chinese with English abstract). *Acta Scientiae Circumstantiae*, 27, 817–823.

Zhai, W. D., & Dai, M. H. (2009). On the seasonal variation of air–sea CO₂ fluxes in the outer Changjiang (Yangtze River) Estuary, East China Sea. *Marine Chemistry*, 117(1–4), 2–10. <https://doi.org/10.1016/j.marchem.2009.02.008>

Zhang, L., Xue, M., Wang, M., Cai, W. J., Wang, L., & Yu, Z. (2014). The spatiotemporal distribution of dissolved inorganic and organic carbon in the main stem of the Changjiang (Yangtze) river and the effect of the Three Gorges Reservoir. *Journal of Geophysical Research: Biogeosciences*, 119, 741–757. <https://doi.org/10.1002/2012JG002230>